J IRAN CHEM SOC (2016) 13:323–330
DOI 10.1007/s13738-015-0740-7

ORIGINAL PAPER

Electrochemistry and electrocatalysis of myoglobin on electrodeposited ZrO_2 and graphene-modified carbon ionic liquid electrode

Wencheng Wang[1] · Xiaoqing Li[2] · Xiaohua Yu[2] · Lijun Yan[1] · Bingxin Lei[1] · Pan Li[1] · Changxing Chen[1] · Wei Sun[1]

Received: 9 March 2015 / Accepted: 15 September 2015 / Published online: 23 September 2015

Abstract In this paper, an electrodeposited zirconia (ZrO_2) nanoparticle and graphene (GR) nanosheet-modified carbon ionic liquid electrode (CILE) was fabricated to get a modified electrode that denoted as ZrO_2/GR/CILE, which was further used for the immobilization of myoglobin (Mb). The performances of ZrO_2/GR/CILE were checked by scanning electron microscopy and electrochemical methods, and the results indicated the formation of nanocomposite on the electrode surface with increased surface area. Direct electrochemistry of Mb was realized on the modified electrode with a pair of well-defined quasi-reversible redox peaks appeared, which was ascribed to the typical electrochemical behaviors of Mb Fe(III)/Fe(II) redox couples. Therefore, the presence of ZrO_2/GR on the electrode could provide a specific interface for accelerating the electron transfer of Mb with the underlying electrode. Electrochemical behaviors of Mb were carefully investigated with the electrochemical parameters calculated. Under the selected conditions, the Mb-modified electrode exhibited excellent electrocatalytic activity to the reduction of trichloroacetic acid in the concentration range from 0.4 to 29.0 mmol L^{-1} with a detection limit of 0.13 mmol L^{-1} (3σ).

Keywords Graphene · Zirconia nanoparticle · Myoglobin · Direct electrochemistry · Electrocatalysis

Introduction

Direct electrochemistry between redox proteins with electrodes is of great interests due to its fundamental significance in electron transfer mechanism of the biological system and practical applications in biosensors, biofuel cells and related biodevices [1, 2]. However, due to the deep embedment of electroactive center in the protective matrix of protein, direct electron transfer of redox proteins with traditional electrodes is difficult to be realized. Therefore, different kinds of chemically modified electrodes have been devised for the realization of electron transfer [3, 4]. In recent years, nanosized materials with various morphography have been applied to the protein electrochemistry. The presence of nanomaterials can shorten the distances between redox active center and electrode with a biocompatible interface suitable for the orientation of proteins. Therefore, the direct electron transfer of redox proteins could be easily realized on the nanoparticles modified electrodes [5, 6].

As a two-dimensional carbon material consisted of sp^2 hybridized carbon atom, graphene (GR) nanosheets have been the research topics in different fields [7–9]. GR has exhibited many advantages including large surface area, excellent electrical conductivity and good biocompatibility. Several groups have reviewed the recent progresses of GR in the fields of electrochemistry and electrochemical sensors [10–12]. In addition, two-dimensional structure of GR nanosheets can be used as the basic building unit for the further construction of GR based nanocomposite [13]. Bai et al. presented a review about the synthesis and application

Electronic supplementary material The online version of this article (doi:10.1007/s13738-015-0740-7) contains supplementary material, which is available to authorized users.

✉ Wei Sun
swyy26@hotmail.com

[1] College of Chemistry and Chemical Engineering, Hainan Normal University, Haikou 571158, China

[2] College of Acumox and Tuina, Shangdong University of Traditional Chinese Medicine, Jinan 250355, China

of GR-inorganic nanocomposites [14]. The presence of various nanomaterials on the surface of GR nanosheets can result in specific hybrids with multi-functions, which have been widely used in electrochemical sensors. For example, Baby et al. fabricated metal decorated GR nanosheets for amperometric glucose sensor [15]. Sun et al. investigated the direct electrochemistry of hemoglobin on GR and titanium dioxide nanorods composite modified electrode [16]. Direct electrochemistry and electrocatalysis of myoglobin (Mb) was also realized on nickel oxide and GR nanocomposite modified electrode [17]. Guo et al. developed a one-pot rapid synthesis method to assemble Pt nanoparticles on the GR nanosheets for electrochemical sensing [18].

As an inorganic oxide with the properties, such as thermal stability, chemical inertness, resistance to poisoning, strong affinity for phosphoric group, large surface area, lack of toxicity and affinity for oxygen-containing groups, zirconia (ZrO_2) has been used in the electrode modification [19]. Due to the high affinity to phosphoric moieties, ZrO_2-based electrode had been used for the detection of phosphopeptide, phosphorprotein and organophosphate pesticides. Liu et al. applied ZrO_2 nanoparticles as selective sorbents for the electrochemical detection of organophosphate pesticides and nerve agents [20]. Du et al. developed a ZrO_2 nanoparticles modified electrode for the sensitive stripping voltammetric detection of organophosphate compounds [21]. Pang et al. synthesized ZrO_2 nanostructures on graphene oxide and further used for selective capture of phosphopeptides [22]. Du et al. described a one-step electrodeposition method for GR-ZrO_2 nanocomposite modified glassy carbon electrode and used for the detection of organophosphorus agents [23]. ZrO_2 modified electrode can also be used for the fabrication of electrochemical DNA sensors due to its strong affinity with the phosphate groups present at the 5′ end of ssDNA probes. Yang et al. used an electrodeposited ZrO_2 composite film modified electrode based electrochemical DNA sensor for the detection of PAT gene fragment [24]. Gong et al. proposed a one-step co-electrodeposition of ZrO_2 nanoparticles decorated GR hybrid nanosheets for an enzymeless parathion sensor [25]. Sun et al. also applied a GR-ZrO_2 nanocomposite modified electrode for the simultaneous electrochemical determination of guanosine and adenosine [26]. Zong et al. prepared a ZrO_2-grafted collagen for the immobilization of redox proteins and applied to unmediated biosensing of H_2O_2 [27]. Liu et al. fabricated an amperometric biosensor based on a nanoporous ZrO_2 matrix for the immobilization of horseradish peroxidase [28]. Zhao et al. investigated the direct electrochemistry and electrocatalysis of heme proteins immobilized on self-assembled ZrO_2 film [29]. Qiao et al. realized the direct electron transfer of Mb in LBL films assembled with poly(ethylene glycol) and ZrO_2 nanoparticles [30]. Liang et al. studied the direct electrochemistry of Mb immobilized on ZrO_2/multi-walled carbon nanotube nanocomposite [31]. Ruan et al. applied the ZrO_2 and IL composite for the investigation on the direct electrochemistry of Mb [32]. However, no references about the application of ZrO_2/GR composite for the direct electrochemistry of redox proteins were reported. Because ZrO_2 nanoparticles have good biocompatibility, and can retain the native structure and bioactivity of biomacromolecules, which is ideal for immobilizing the biomolecules containing oxygen groups. In addition, GR nanosheets can be used for the loading of ZrO_2 nanoparticles with large surface area and high conductivity. Therefore, ZrO_2/GR nanocomposite are chosen for the investigation on the direct electrochemistry of heme proteins.

In this paper an N-hexylpyridinium hexafluorophosphate ($HPPF_6$) based carbon ionic liquid electrode (CILE) was fabricated and used as the substrate electrode for the further modification. By incorporating ionic liquid (IL) in the traditional used carbon paste electrode (CPE), CILE had been proved to exhibit many advantages such as high ionic conductivity, wide electrochemical windows, good electrocatalytic activity, low cost, easy to preparation, high conductivity, anti-fouling effect and renewable surface [33]. GR nanosheets were casted on the CILE surface and further decorated with ZrO_2 nanoparticles by a facile electrodeposition of $ZrOCl_2$. The fabricated ZrO_2/GR/CILE can be served as a good platform for the immobilization of Mb, and direct electrochemistry of Mb was realized on the modified electrode with a pair of well-defined redox peaks appeared. This Mb-modified electrode exhibited excellent electrocatalytic activity to the reduction of trichloroacetic acid (TCA), which could be served as a candidate for the third-generation electrochemical sensor without mediator.

Experimental

Reagents

$HPPF_6$ (>99 %, Lanzhou Greenchem. ILS. LICP. CAS., China), horseheart Mb (MW. 17800, Sigma), GR (Taiyuan Tanmei Ltd. Co., China), chitosan (CTS, minimum 95 % deacetylated, Dalian Xindie Chem. Reagents Ltd. Co., China), graphite powder (average particle size 30 μm, Shanghai Colloid Chem. Ltd. Co., China) and TCA (Tianjin Kemiou Chem. Ltd. Co., China) were used as received. 0.1 mol L^{-1} phosphate buffer solutions (PBS) were used

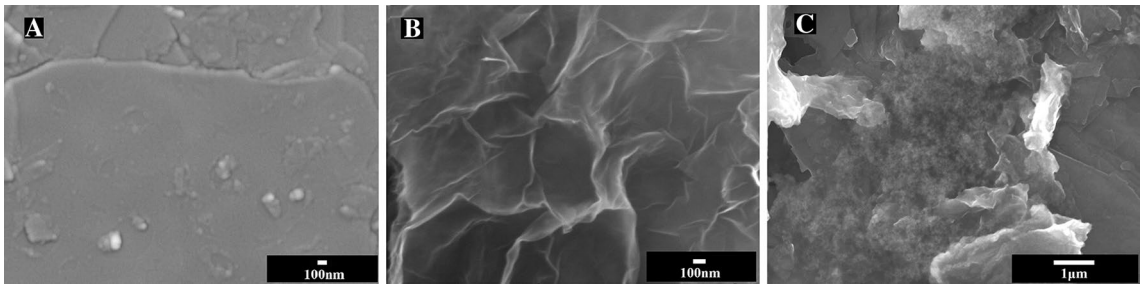

Fig. 1 SEM images of **a** CILE, **b** GR/CILE and **c** ZrO_2/GR/CILE

as the supporting electrolyte. All the other chemicals used were of analytical reagent grade and doubly distilled water was used for all aqueous solutions.

Apparatus

A CHI 750B electrochemical workstation (Shanghai CH Instrument, China) was used for the electrochemical measurements. A conventional three-electrode system was used with a modified CILE as working electrode, a platinum wire as auxiliary electrode and a saturated calomel electrode (SCE) as reference electrode. Scanning electron microscopy (SEM) was performed on a JSM-7100F scanning electron microscope (Japan Electron Company, Japan).

Fabrication of the CTS/Mb/ZrO_2/GR/CILE

CILE was fabricated by hand-mixing 0.80 g of $HPPF_6$ and 1.60 g of graphite powder in a mortar thoroughly. A portion of resulting homogeneous paste was packed firmly into a glass tube ($\Phi = 4$ mm). The electrical contact was established through a copper wire to the end of the paste in the inner hole of the tube. Prior to use a mirror-like surface was obtained by polishing the CILE surface on a weighing paper.

The GR-modified CILE (GR/CILE) was prepared by simply applying 10.0 μL of 1.0 mg mL^{-1} GR suspension ethanol solution on the surface of CILE and left it to dry at the room temperature. Then cyclic voltammetry was employed for the electrodeposition of ZrO_2 nanoparticles onto the surface of GR/CILE with a mixture solution containing 5.0 mmol L^{-1} $ZrOCl_2$ and 0.1 mol L^{-1} KCl. The potential range for multiple-scan cyclic voltammetric experiment was from −1.1 to 0.7 V with a scan rate of 20 mV s^{-1} and a scan number of 10. The fabricated ZrO_2/GR/CILE was rinsed by water and dried in air. Then 10.0 μL of 20.0 mg mL^{-1} Mb solution was dropped on the surface of ZrO_2/GR/CILE and stayed silent to allow the water evaporated gradually. At last 10.0 μL of 1.0 mg mL^{-1} CTS (1.0 % HOAc) solution was cast on the surface of Mb/ZrO_2/GR/CILE to form a stable film. The resulted CTS/Mb/ZrO_2/GR/CILE was stored at 4 °C in a refrigerator under dry conditions when not in use.

Voltammetric measurements

Electrochemical measurements were carried out in a 10.0 mL electrochemical cell containing 0.1 mol L^{-1} pH 6.0 PBS at room temperature. The working buffer solutions were deoxygenated by bubbling high pure nitrogen thoroughly for at least 30 min just before the electrochemical experiments and the nitrogen atmosphere environment was kept in the electrochemical cell during the measurements.

Results and discussion

SEM of the modified electrodes

SEM images of different modified electrodes were recorded with the results shown in Fig. 1. On CILE a flat surface appeared (Fig. 1a), which could be attributed to the high viscosity of IL that could bind the graphite powder together and fill into the void space of graphite powder. On GR/CILE (Fig. 1b) the specific appearance of GR nanosheets could be observed with the sheet-like structures, which indicated that GR nanosheets were present on the CILE surface. After electrodeposition of ZrO_2 on the surface of GR/CILE (Fig. 1c), ZrO_2 nanoparticles could be found on the GR nanosheets. Electrodeposition is a facile and controllable procedure for the synthesis of ZrO_2 nanoparticles with green nature, which has been widely used for the preparation of ZrO_2 on different matrix [34]. By using GR/CILE as the substrate electrode, nanosized ZrO_2 could be directly formed on the GR surface to get a composite, which increased the roughness of the interface and could be used for the further modification.

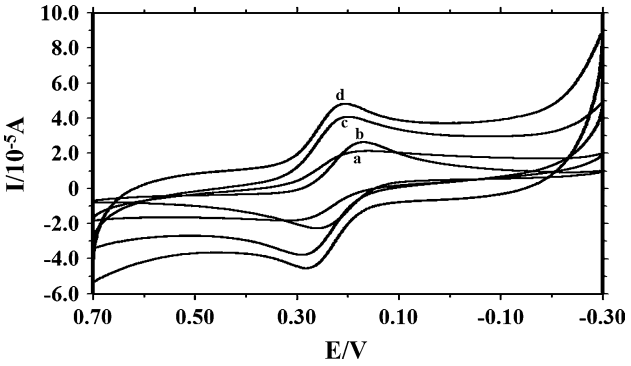

Fig. 2 Cyclic voltammograms of **a** ZrO_2/CILE, **b** CILE, **c** ZrO_2/GR/CILE and **d** GR/CILE in a 1.0 mmol L^{-1} $K_3[Fe(CN)_6]$ and 0.5 mol L^{-1} KCl solution with the scan rate of 100 mV s^{-1}

conductivity, which is benefit for electrochemical applications [7]. With the further deposition of ZrO_2 on GR/CILE the redox peak current decreased (curve c), indicating the successful formation of ZrO_2 nanoparticles on the GR surface. The effective electrode surface (A) was further calculated by cyclic voltammetric method based on changing scan rate and recording the redox peak currents. Based on the Randles–Servick equation:

$$\mathrm{Ipc} = \left(2.69 \times 10^5\right) n^{2/3} A D^{1/2} C * \upsilon^{1/2}$$

where Ipc is the reduction peak current (A), n is the electron transfer number, A is the effective surface area (cm^2), D is the diffusion coefficient of $K_3[Fe(CN)_6]$ in the solution (cm^2 s^{-1}), C^* is the concentration of $K_3[Fe(CN)_6]$ (mol L^{-1}) and v is the scan rate (V s^{-1}), then A value of ZrO_2/GR/CILE were calculated as 0.0930 cm^2.

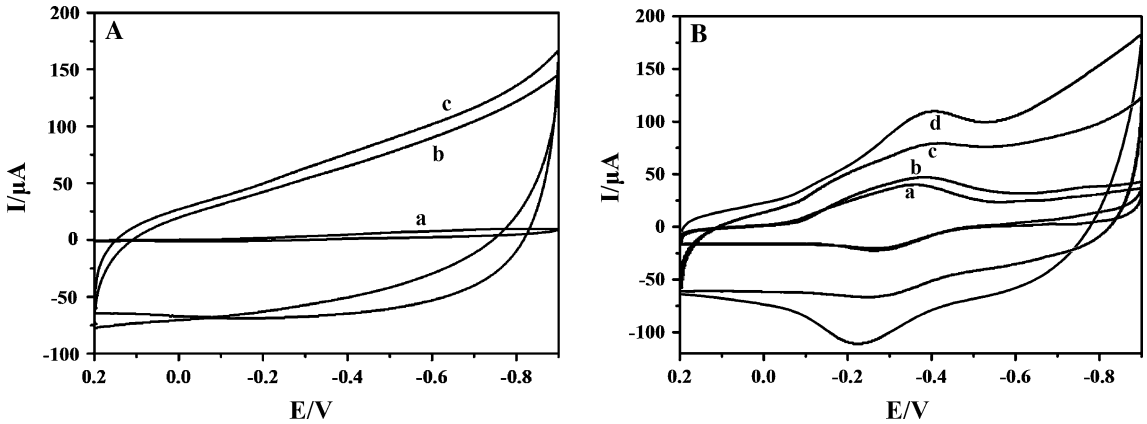

Fig. 3 **a** Cyclic voltammograms of **a** CILE, **b** ZrO_2/GR/CILE and **c** GR/CILE in pH 6.0 PBS at the scan rate of 100 mV s^{-1}; **b** cyclic voltammograms of **a** CTS/Mb/CILE, **b** CTS/Mb/ZrO_2/CILE, **c** CTS/Mb/GR/CILE and **d** CTS/Mb/ZrO_2/GR/CILE in pH 6.0 PBS at the scan rate of 100 mV s^{-1}

Electrochemical performances of the modified electrodes

Cyclic voltammetric curves of different modified electrodes in a 1.0 mmol L^{-1} $[Fe(CN)_6]^{3-/4-}$ solution were recorded and shown in Fig. 2. It can be seen that a pair of redox peaks appeared on all the modified electrodes and the electrochemical data were listed in table S1. On CILE a pair of well-defined redox peak appeared (curve b), which could be attributed to the conductive IL present in the carbon paste. After the deposition of ZrO_2 nanoparticles the redox peak currents on ZrO_2/CILE (curve a) was smaller than that of CILE (curve b), indicating the presence of semiconductive ZrO_2 nanoparticles on the surface of CILE hindered the electron transfer. While on GR/CILE the biggest redox peak currents appeared (curve d), indicating the presence of GR nanosheets on the CILE surface resulted in the great increase of electrochemical responses. GR nanosheets exhibit the properties including large surface area and high

Direct electrochemistry of different modified electrodes

Figure 3 showed cyclic voltammograms of different modified electrodes in a pH 6.0 PBS at the scan rate of 100 mV s^{-1}. As shown in Fig. 3a, no obvious redox peaks appeared on CILE (curve a), ZrO_2/GR/CILE (curve b) and GR/CILE (curve c), indicating these electrodes were stable in the selected potential range. The increase of the background currents were attributed to the presence of the nanomaterials that increased the interfacial capacitance currents. After the incorporation of Mb molecules on the surface of different modified electrodes, a pair of redox peaks appeared (Fig. 3b), which indicated that direct electron transfer of Mb was realized on different substrate electrode. On CTS/Mb/CILE, the curve was not symmetry

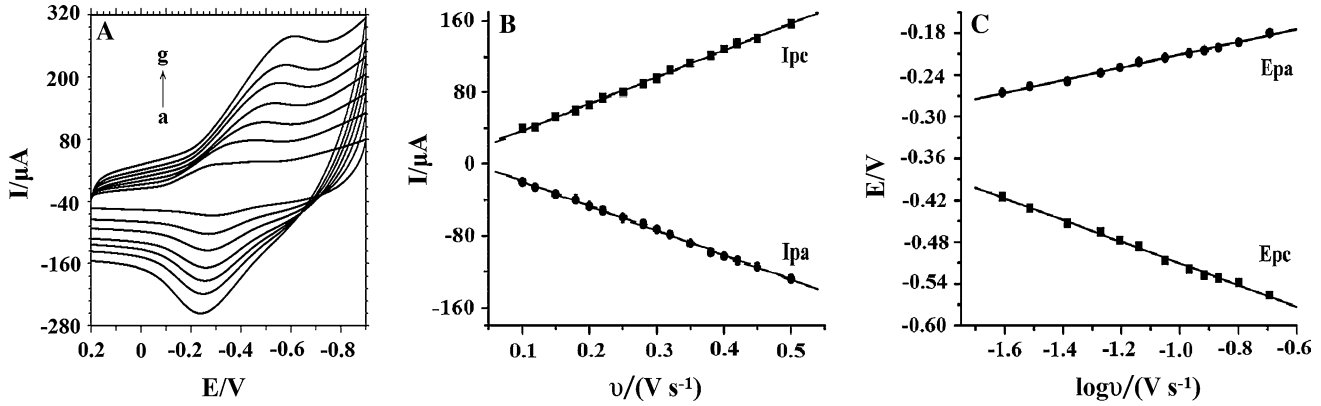

Fig. 4 **a** Cyclic voltammograms of CTS/Mb/ZrO_2/GR/CILE with different scan rates (from **a** to **g** as 50, 100, 150, 200, 250, 300, 380 mV s^{-1}) in pH 6.0 PBS; **b** linear relationship of cathodic and anodic peak current (Ip) vs. scan rate (υ); **c** linear relationship of the redox peak potential vs. logυ

with smallest redox peak currents (curve a), and the electrochemical responses increased a little on CTS/Mb/ZrO_2/CILE (curve b), indicating the presence of ZrO_2 nanoparticles could facilitate the electron transfer. While on CTS/Mb/GR/CILE the redox response also increased (curve c), indicating the presence of GR nanosheet was benefit for the electron transfer of Mb. While on CTS/Mb/ZrO_2/GR/CILE the biggest redox peak currents appeared with almost symmetric peak shape (curve d). The presence of ZrO_2/GR nanocomposite on the electrode surface can provide a specific interface for the immobilization of Mb molecules. GR exhibits high conductivity with large surface area, which is suitable for the further deposition of other kinds of nanoparticles. While ZrO_2 nanoparticles exhibit excellent biocompatibility with oxygenal groups existed, which can modulate the interface with good hydrophilicity [31]. Therefore, Mb on the ZrO_2/GR nanocomposite modified electrode can easily exchange electrons with the basal electrode. From curve d, the values of cathodic peak potential (Epc) and anodic peak potential (Epa) were got as at −0.226 and −0.385 V, respectively. The formal peak potential ($E^{0\prime}$), which is calculated from the midpoint of Epa and Epc with the equation as $E^{0\prime} = (\text{Epa} + \text{Epc})/2$, was estimated as −0.306 V (vs. SCE). The result was the typical characteristic of electroactive heme Fe(III)/Fe(II) redox couples. Therefore, direct electron transfer of Mb was successfully accelerated on ZrO_2/GR nanocomposite modified electrode.

Effect of scan rate

The influence of scan rate (υ) on the electrochemical responses of CTS/Mb/ZrO_2/GR/CILE was further investigated by cyclic voltammetry with the results shown in Fig. 4a. With the increase of scan rate in the range from 0.5 to 500 mV s^{-1}, the redox peak currents increased gradually with a pair of symmetric redox peaks appeared. Good linear relationships were calculated with two linear regression equations as Ipc (10^{-5} A) = 30.02υ (V s^{-1}) + 0.728 (n = 16, γ = 0.999) and Ipa (10^{-5} A) = −27.45 υ (V s^{-1}) + 0.831 (n = 16, γ = 0.999), respectively (Fig. 4b). The results indicated that the electrochemical behavior of Mb immobilized on the modified electrode was a surface-controlled thin-layer process, in which the electroactive Mb Fe(III) in the film were reduced to Mb Fe(II) on the forward cyclic voltammetric scan and then fully reoxidized to Mb Fe(III) on the reversed scan.

With the increase of scan rate the redox peak potentials changed gradually with the peak-to-peak separation (ΔEp) enlarged, which indicated a quasi-reversible electrochemical process. Then the electrochemical parameters were calculated according to the model of Laviron's equations [35, 36]:

$$\text{Epc} = E^{0'} - \frac{2.3\text{RT}}{\alpha nF}\log\upsilon \tag{1}$$

$$\text{Epa} = E^{0'} + \frac{2.3\text{RT}}{(1-\alpha)nF}\log\upsilon \tag{2}$$

$$\log k_s = \alpha\log(1-\alpha) + (1-\alpha)\log\alpha - \log\frac{RT}{nFv} - \frac{(1-\alpha)\alpha Fn\Delta Ep}{2.3\text{RT}} \tag{3}$$

where α is the electron transfer coefficient, k_s is the apparent heterogeneous electron transfer rate constant, R is the gas constant and T is the absolute temperature. Two straight lines were got with the equations as Epc(V) = –0.156 logυ − 0.667 (n = 12, γ = 0.998) and Epa(V) = 0.0907 logυ − 0.120 (n = 12, γ = 0.997) (Fig. 4c). Then the values of α, n and k_s were calculated as 0.368, 1.03 and 3.76 s^{-1},

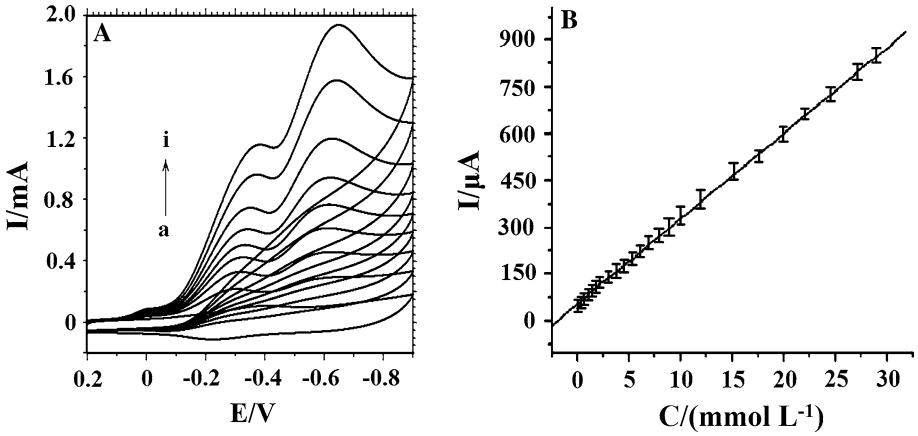

Fig. 5 **a** Cyclic voltammograms of CTS/Mb/ZrO_2/GR/CILE with 0, 2.0, 3.0, 5.0, 7.0, 9.0, 12.0, 20.0, 29.0 mmol L^{-1} TCA (curves **a**–**i**) in 0.1 mol L^{-1} pH 6.0 PBS at the scan rate of 100 mV s^{-1}; **b** linear relationship of catalytic reduction peak currents and the TCA concentration

respectively. It is well known that k_s reflects the local microenvironment of the protein immobilized on the electrode and the value obtained here is in the range of k_s for a typical surface-controlled quasi-reversible electron transfer process. This k_s value is higher that of Mb immobilized on Ag-CNTs/GCE (0.41 s^{-1}) [37], MWCNT/CILE (0.332 s^{-1}) [38], GR-Pt nanocomposite/CILE (0.584 s^{-1}) [39], and nanoporous ZnO/graphite electrode (1.0 s^{-1}) [40]. Therefore, the electron transfer of Mb was facile due to the specific microenvironment provided by ZrO_2/GR composite.

By integrating cyclic voltammetric reduction peaks, the surface concentration (Γ^*) of electroactive Mb on the electrode can be calculated from the following equation: $Q = nFA\Gamma^*$ [41], where Q is charge passing through the electrode with full reduction of electroactive Mb, n is the number of electron transferred, F is the Faraday's constant, A is the effective area of the nanocomposite modified electrode ($A = 0.0930$ cm^2). Then the value of Γ^* was got as 2.55×10^{-9} mol cm^{-2}, which was much larger than the theoretical monolayer coverage of 1.89×10^{-11} mol cm^{-2} [42]. The result also demonstrated that ZrO_2/GR composite provided a suitable interface for multi-layers of Mb on the electrode with suitable orientation to exchange electrons with the basal electrode. While the total amounts of Mb cast on the electrode surface, which was calculated based on the concentration and volume of Mb casted on the electrode surface, was got as 3.30×10^{-8} mol cm^{-1}. Therefore, the fraction of electroactive proteins among the total proteins on CILE surface was got as 7.96 %.

Effect of buffer pH

In most cases, the electrochemical behaviors of redox proteins are significantly dependent on the pH of buffer solution. Therefore, the effect of buffer pH on the electrochemical responses of CTS/Mb/ZrO_2/GR/CILE was investigated in the pH range of 3.0–9.0 by cyclic voltammetry. The results indicated that the buffer pH had greatly influence on the responses with the cyclic voltammgrams deformed as the pH of buffer increased. In addition, the redox peak potentials moved to the negative direction with the increase of the buffer pH, indicating that protons were involved in the electrode reaction. The formal peak potential ($E^{0\prime}$) had a good linear relationship with the buffer pH and the linear regression equation was calculated as $E^{0\prime}(V) = -0.0574$ pH + 0.0246 ($n = 13$, $\gamma = 0.998$). The slope value of −57.4 mV pH^{-1} was reasonably close to the theoretical value of −59.0 mV pH^{-1} at 25 °C for a reversible one proton coupled with one electron redox reaction process [41], so the electrochemical reaction of Mb on the electrode can be expressed as Mb Fe(III) + H^+ + e Mb Fe(II). In addition, the biggest redox peak current appeared at pH 6.0 buffer solution, which was selected for the further electrochemical experiments.

Electrocatalytic activity

Redox proteins film modified electrode had exhibited excellent catalytic properties to the reduction of organohalides, therefore they can be employed to determine and destroy organohalides, such as TCA, benzene hexachloride and perchloroethylene [43]. Due to the presence of Mb on the electrode surface, CTS/Mb/ZrO_2/GR/CILE showed good electrocatalytic ability to the reduction of TCA. As shown in Fig. 5a, an increase of the reduction peak current was observed at −0.323 V (vs. SCE) after the addition of different concentration of TCA into pH 6.0 PBS. At the same time, the oxidation peak of Mb Fe(III) decreased and disappeared, which may be due to the oxidation of Mb Fe(II) to Mb Fe(III) by TCA. With the further increase of the TCA concentration another new reduction peak appeared at −0.657 V. This peak could be attributed to the formation of a highly reduced form of Mb [Mb Fe(I)], which might dechlorinate di- and mono-chloroacetic acid after the dechlorination of TCA with Mb Fe(II) [44]. The catalytic reduction peak current increased with the TCA

Table 1 Comparison of the analytical parameters for the electrochemical detection of TCA

Modified electrodes	Linear range (mmol L^{-1})	Detection limit (mmol L^{-1})	References
Nafion/Mb/MWCNT/CILE	1.57–12.0	0.1	[38]
Nafion/Mb-GR-Pt/CILE	0.9–9.0	0.32	[39]
Nafion/Mb/Co/CILE	0.4–12.0	0.2	[45]
CTS/Mb–Fe_3O_4@SiO_2/CILE	0.2–11.0	0.18	[46]
$\{PDDA/Hb\}_8$/PGE	3.92–58.4	1.98	[47]
Hb/Fe_3O_4/PIGE	5.0–65.4	0.116	[48]
Nafion/Mb/Au/GR/CILE	0.4–20.0	0.13	[49]
Mb/DNA/CILE	0.5–40.0	0.083	[50]
CTS/Mb/ZrO_2/GR/CILE	0.4–29.0	0.13	This work

concentration in the range from 0.4 to 29.0 mmol L^{-1} and the linear regression equation was got as $I_{ss}(\mu A) = 27.39$ C (mmol L^{-1}) + 51.09 ($n = 28$, $\gamma = 0.997$) (shown in Fig. 5b) with the detection limit as 0.13 mmol L^{-1} (3σ). A comparison of the analytical parameters for the electrochemical detection of TCA by different kinds of redox protein modified electrodes was summarized in Table 1. It can be seen that this method had relatively wider linear range and lower detection limit. When the TCA concentration was more than 29.0 mmol L^{-1}, the reduction peak current turned to level off, indicating a typical Michaelis–Menten kinetic process. According to the Lineweaver–Burk equation [51], $1/I_{ss} = (1/I_{max})\ (1 + K_M^{app}/C)$, where I_{ss} is the steady current after the addition of substrate, C is the bulk concentration of the substrate, and I_{max} is the maximum current measured under saturated substrate condition. So the apparent Michaelis–Menten constant (K_M^{app}) was calculated to be 1.895 mmol L^{-1}, which was smaller than that of some previous reported values such as 5.13 mmol L^{-1} on agarose/GCE [42], 10.67 mmol L^{-1} on Nafion/Mb/NiO/GR/CILE [17], and 15.47 mmol L^{-1} on Nafion/Au/GR/CILE [49]. The lower K_M^{app} value indicated that Mb immobilized on the modified electrode retained its bioactivity and had a high biological affinity to TCA.

Reproducibility and stability

The reproducibility of CTS/Mb/ZrO_2/GR/CILE was assessed by measuring the current response of the modified electrode to 6.0 mmol L^{-1} TCA with the average relative standard deviation (RSD) lower than 3.2 %. Ten modified electrodes were prepared in the same procedure and used for the detection of 6.0 mmol L^{-1} TCA with a RSD value of 3.6 % obtained, indicating the high repeatability of this preparation procedure. To investigate the stability of the modified electrode, the current response to 6.0 mmol L^{-1} of TCA was recorded every week. After 4 weeks of storage, the current response was still remained 93.8 % of its original signal, which demonstrated the long-term stability of the modified electrode.

Conclusions

In this article, an IL $HPPF_6$-based CILE was fabricated and used as the basal electrode. Then GR nanosheets and ZrO_2 nanoparticles were modified on the CILE surface step-by-step to get ZrO_2/GR/CILE. Mb was further cast on ZrO_2/GR/CILE with a CTS film to fix the Mb molecules tightly on the electrode surface. Cyclic voltammetric results indicated that a pair of well-defined redox peaks appeared, indicated that direct electrochemistry of Mb was achieved in the composite film. Electrocatalysis of CTS/Mb/ZrO_2/GR/CILE toward TCA was further investigated with satisfactory result. Therefore, the ZrO_2/GR nanocomposite may have potential applications in constructing electrochemical biosensors based on mediator-free electrochemistry of the redox enzymes.

Acknowledgments We acknowledge the financial support from the National Natural Science Foundation of China (Nos. 21365010, 51363008), the Nature Science Foundation of Hainan Province (20152016), the Science and Technology Cooperation Project of Hainan Province (KJHZ2015-13) and Graduate Student Innovation Research Projects of Hainan Normal University.

References

1. F.A. Armstrong, H.A.O. Hill, N.J. Walton, Acc. Chem. Res. **21**, 407 (1988)
2. J.F. Rusling, Acc. Chem. Res. **31**, 363 (1998)
3. F.A. Armstrong, G.S. Wilson, Electrochim. Acta **45**, 2623 (2000)
4. E. Lojou, P. Bianco, Electroanalysis **16**, 1113 (2004)
5. Y. Liu, Y. Du, C.M. Li, Electroanalysis **25**, 815 (2013)
6. C.Z. Zhu, G.H. Yang, H. Li, D. Du, Y.H. Lin, Anal. Chem. **87**, 230 (2015)
7. D. Chen, H.B. Feng, J.H. Li, Chem. Rev. **112**, 6027 (2012)
8. C. Li, G.Q. Shi, Adv. Mater. **26**, 3992 (2014)
9. I.V. Pavlidis, M. Patila, U.T. Bornscheuer, D. Gournis, H. Stamatis, Trends Biotechnol. **32**, 312 (2014)
10. Y.Y. Shao, J. Wang, H. Wu, J. Liu, I.A. Aksay, Y.H. Lin, Electroanalysis **22**, 2010 (1027)
11. G. Jo, M. Choe, S. Lee, W. Park, Y.H. Kahng, T. Lee, Nanotechnology **23**, 112001 (2012)
12. D. Chen, L.H. Tang, J.H. Li, Chem. Soc. Rev. **39**, 3157 (2010)

13. V. Singh, D. Joung, L. Zhai, S. Das, S.I. Khondaker, S. Seal, Prog. Mater Sci. **56**, 1178 (2011)
14. S. Bai, X.P. Shen, RSC Adv. **2**, 64 (2012)
15. T.T. Baby, S.S. Aravind, T. Arockiadoss, R.B. Rakhi, S. Ramaprabhu, Sens. Actuators B: Chem. **145**, 71 (2010)
16. W. Sun, Y.Q. Guo, X.M. Ju, Y.M. Zhang, X.Z. Wang, Z.F. Sun, Biosens. Bioelectron. **42**, 207 (2013)
17. W. Sun, S.X. Gong, Y. Deng, T.T. Li, Y. Cheng, W.C. Wang, L. Wang, Thin Solid Films **562**, 653 (2014)
18. S.J. Guo, D. Wen, Y.M. Zhai, S.J. Dong, E.K. Wang, ACS Nano **4**, 3959 (2010)
19. F. Bellezza, A. Cipiciani, M.A. Quotadamo, Langmuir **21**, 11099 (2005)
20. G.D. Liu, Y.H. Lin, Anal. Chem. **77**, 5894 (2005)
21. D. Du, X.P. Ye, J.D. Zhang, Y. Zeng, H.Y. Tu, A.D. Zhang, D.L. Liu, Electrochem. Commun. **10**, 686 (2008)
22. H. Pang, Q.Y. Lu, F. Gao, Chem. Commun. **47**, 11772 (2011)
23. D. Du, J. Liu, X.Y. Zhang, X.L. Cui, Y.H. Lin, J. Mater. Chem. **21**, 8032 (2011)
24. J. Yang, K. Jiao, T. Yang, Anal. Bioanal. Chem. **389**, 913 (2007)
25. J.M. Gong, X.J. Miao, H.F. Wang, D.D. Song, Sens. Actuator B Chem. **102**, 341 (2012)
26. W. Sun, X.Z. Wang, X.H. Sun, Y. Deng, J. Liu, B.X. Lei, Z.F. Sun, Biosens. Bioelectron. **44**, 146 (2013)
27. S.Z. Zong, Y. Cao, Y.M. Zhou, H.X. Ju, Langmuir **22**, 8915 (2006)
28. B.H. Liu, Y. Cao, D.D. Chen, J.L. Kong, J.Q. Deng, Anal. Chim. Acta **478**, 59 (2003)
29. G. Zhao, J.J. Feng, J.J. Xu, H.Y. Chen, Electrochem. Commum. **7**, 724 (2009)
30. K. Qiao, N.F. Hu, Bioelectrochemistry **75**, 71 (2009)
31. P. Liang, M.Q. Deng, S.G. Cui, H. Chen, J.D. Qiu, Mater. Res. Bull. **45**, 1855 (2010)
32. C.X. Ruan, T.T. Li, X.M. Ju, H.J. Liu, J. Lou, W.M. Gao, W. Sun, J. Solid State Electrochem. **16**, 3661 (2012)
33. M. Opallo, A. Lesniewski, J. Electroanal. Chem. **656**, 2 (2011)
34. N.N. Zhu, A.P. Zhang, Q.J. Wang, P.G. He, Y.Z. Fang, Anal. Chim. Acta **510**, 163 (2004)
35. E. Laviron, J. Electroanal. Chem. **52**, 355 (1974)
36. E. Laviron, J. Electroanal. Chem. **101**, 19 (1979)
37. C.Y. Liu, J.M. Hu, Biosens. Bioelectron. **24**, 2149 (2009)
38. W. Sun, X.Q. Li, Y. Wang, X. Li, C.Z. Zhao, K. Jiao, Bioelectrochemistry **75**, 170 (2009)
39. W. Sun, L.F. Li, B.X. Lei, T.T. Li, X.M. Ju, X.Z. Wang, G.J. Li, Z.F. Sun, Mater. Sci. Eng., C **33**, 1907 (2013)
40. G. Zhao, J.J. Xu, H.Y. Chen, Anal. Biochem. **350**, 145 (2006)
41. A.J. Bard, L.R. Fulkner, *Electrochemical Methods* (Fundamentals and applications, Wiley, New York, 2001)
42. S.F. Wang, T. Chen, Z.L. Zhang, X.C. Shen, Z.X. Lu, D.W. Pang, K.Y. Wong, Langmuir **21**, 9260 (2005)
43. N.F. Hu, Pure Appl. Chem. **72**, 1979 (2001)
44. C.H. Fan, Y. Zhuang, G.X. Li, Q.J. Zhu, D.X. Zhu, Electroanalysis **12**, 1156 (2000)
45. W. Sun, X.Q. Li, P. Qin, K. Jiao, J. Phys. Chem. **113**, 11294 (2009)
46. X.F. Wang, Z. You, H.L. Sha, Z.L. Sun, W. Sun, J. Solid State Electrochem. **18**, 207 (2014)
47. P.L. He, N.F. Hu, G. Zhou, Biomacromolecules **3**, 139 (2002)
48. J.M. Gong, X.Q. Lin, Microchem. J. **75**, 51 (2003)
49. G.N. Li, T.T. Li, Y. Deng, Y. Cheng, F. Shi, W. Sun, Z.F. Sun, J. Solid State Electrochem. **17**, 2333 (2013)
50. R.F. Gao, J.B. Zheng, Electrochem. Commun. **11**, 1527 (2009)
51. R.A. Kamin, G.S. Wilson, Anal. Chem. **52**, 1198 (1980)